Journal of Materials Chemistry A

Accepted Manuscript

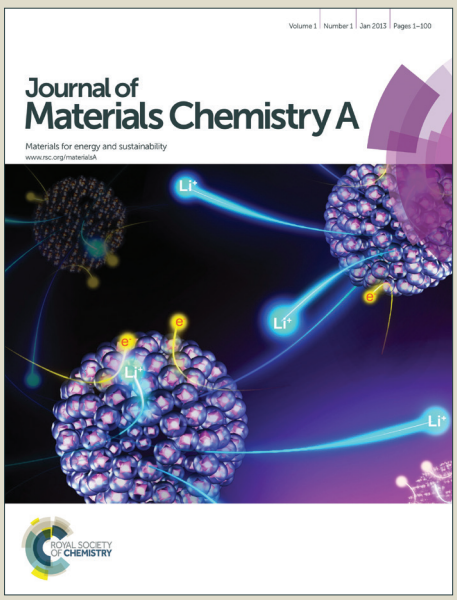

ROYAL SOCIETY OF CHEMISTRY

www.rsc.org/materialsA

Journal Name

RSCPublishing

ARTICLE

Effects of Various π-Conjugated Spacers in Thiadiazole[3,4-*c*]pyridine-Cored Panchromatic Organic Dyes for Dye-Sensitized Solar Cells

Cite this: DOI: 10.1039/x0xx00000x

Received 00th January 2012,
Accepted 00th January 2012

DOI: 10.1039/x0xx00000x

www.rsc.org/

Yong Hua,[§a] Jian He,[§b] CaishunZhang,[c] ChunjiangQin,[d] LiyuanHan,[d] Jianzhang Zhao,[c] Tao Chen,*[b] Wai-Yeung Wong,*[a], Wai-Kwok Wong*[a] and Xunjin Zhu,*[a]

A series of new metal-free panchromatic organic photosensitizers based on a strong electron-deficient thiadiazole[3,4-*c*]pyridine core has been designed and applied in dye-sensitized solar cells. The incorporation of the auxiliary thiadiazole[3,4-*c*]pyridine unit can effectively adjust the HOMO and LUMO energy levels, to design small band-gap sensitizers with panchromatic absorption. The impacts of various π-conjugated spacers on the absorption properties, electrochemical properties and photovoltaic performances have been investigated systematically. The sensitizer **Y3** with a benzene unit adjacent to the anchoring cyanoacrylic group produces a higher photocurrent and photovoltage in cell performance, as compared to **Y1** and **Y2** with thiophene and *n*-hexylthiophene unit adjacent to the anchoring group, respectively. Further structural optimization in **Y4** with a *n*-hexylthiophene π-conjugated spacer inserted between the donor and thiadiazole[3,4-*c*]pyridine core results in the best photovoltaic performance. For comparison, the sensitizer **Y5** with thiophene instead of *n*-hexylthiophene in the molecule exhibits the most inferior performance, which in turn demonstrates that the long alkyl chains can effectively improve the cell performance by suppressing the dye aggregation on TiO_2 film, enhancing electron injection efficiency, and retarding charge recombination by shielding the surface of TiO_2 from the I_3^- ions. The overall conversion efficiency of liquid-electrolyte DSSC based on **Y4** shows the highest efficiency of 6.30% with a short-circuit photocurrent density (J_{sc}) of 12.54 mA cm^{-2}, an open-circuit photovoltage (V_{oc}) of 0.749 V, and a fill factor (FF) of 0.671, under standard global AM 1.5 solar light condition. Density functional theory calculations and electrochemical impedance spectroscopy analysis of these sensitizers provide further insight into the molecular geometry and the impact of the different π-conjugated spacers on the photophysical and photovoltaic performance.

Introduction

Dye-sensitized solar cell (DSSC) has received remarkably attention as an alternative to conventional semi-conductor silicon-based solar cell since the pioneering work reported by Grätzel and O'Regan in 1991,[1] owing to their low production cost and potential mass manufacturing application. In a typical DSSC, the photosensitizer exerts a significant influence on the light-harvesting and power conversion efficiency (PCE). During the past two decades, keen interests have been concentrated on the development of metal-free organic dyes, which have been one of the most promising candidates in DSSCs due to the low material cost, high molecular absorption extinction coefficient, and structural design flexibility.[2-7] However, metal-free organic sensitizers exhibit a relatively poor absorption spectral response in the red and near infrared (NIR) region. One strategy of extending the spectral coverage to enhance the light harvesting efficiency is to reduce the HOMO–LUMO energy gap of sensitizers. For this purpose, a series of D–A–π–A structured sensitizers for DSSCs have been prepared by incorporating electron-deficient fragments into the π-conjugated spacer of organic dyes, such as, benzothiadiazole,[8] quinoxaline,[9] diketopyrrolopyrrole[10] and benzotriazole,[11] which can conveniently tune the molecular

energy gap, modulating the absorption spectral response to match the solar emission spectrum. Moreover, the incorporated electron-deficient fragment was demonstrated to facilitate the electron transfer from the donor to the acceptor end.[12] Thiadiazolo[3,4-*c*]pyridine (PyT), recognized as a strong electron-deficient unit due to its two symmetric unsaturated nitrogen atoms and the pyridine N-atoms, has been widely applied to construct pull-push copolymers with narrow band gaps in the field of bulk heterojunction organic photovoltaics.[13] These materials containing PyT unit display good thermal stability and narrow band gaps, broad optical absorption extending into the NIR region. In our previous work, we developed three D–A–π–A structured panchromatic photosensitizers incorporating PyT unit as an additional acceptor and applied them in DSSCs.[14] As expected, the spectral response of DSSCs based on those three dyes covered the whole visible region and reached above 800 nm. However, the PCEs obtained were lower than 4.20%. A further molecular optimization of these kinds of panchromatic sensitizers based on PyT unit is emerging for achieving superior photovoltaic performance.

In this study, we designed a series of new organic photosensitizers (**Y1–Y5**) incorporating the electron-deficient PyT unit in the framework of π-conjugated spacer, and dihexyloxy-substituted triphenylamine as the donor, cyanoacylic acid as the acceptor and anchoring part (**Figure 1**). And the impacts of various π-conjugated spacers on the absorption properties, electrochemical properties and photovoltaic performances have been investigated systematically. Spectroscopic, electrochemical, theoretical calculation and Electrochemical Impedance Spectroscopies analysis were performed to understand how the subtle structural variations on the sensitizers affect the photovoltaic performance in DSSC.

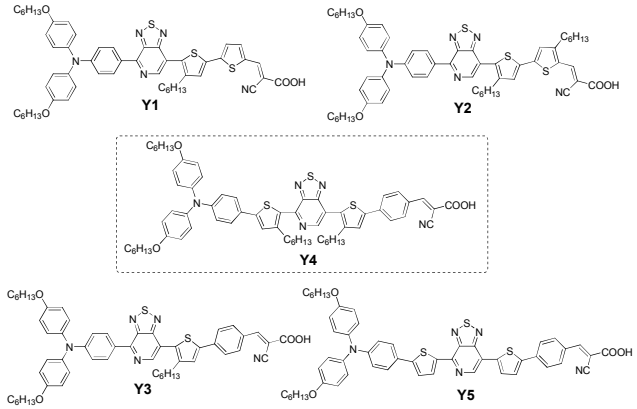

Figure 1. Chemical structures of **Y1–Y5**.

Results and discussion

Synthesis and characterization

The synthetic procedures for sensitizers **Y1–Y5** starting from 4,7-dibromo-[1,2,5]thiadiazolo[3,4-*c*]pyridine are depicted in **Scheme 1**. The key precursors were synthesized according to the literature methods. The target compounds **Y1–Y5** were achieved in moderate yields via bromination, Suzuki cross-coupling reaction and the Knoevenagel condensation. All the new compounds were well characterized by ^{1}H NMR, ^{13}C NMR spectroscopy as well as HRMS spectroscopy.

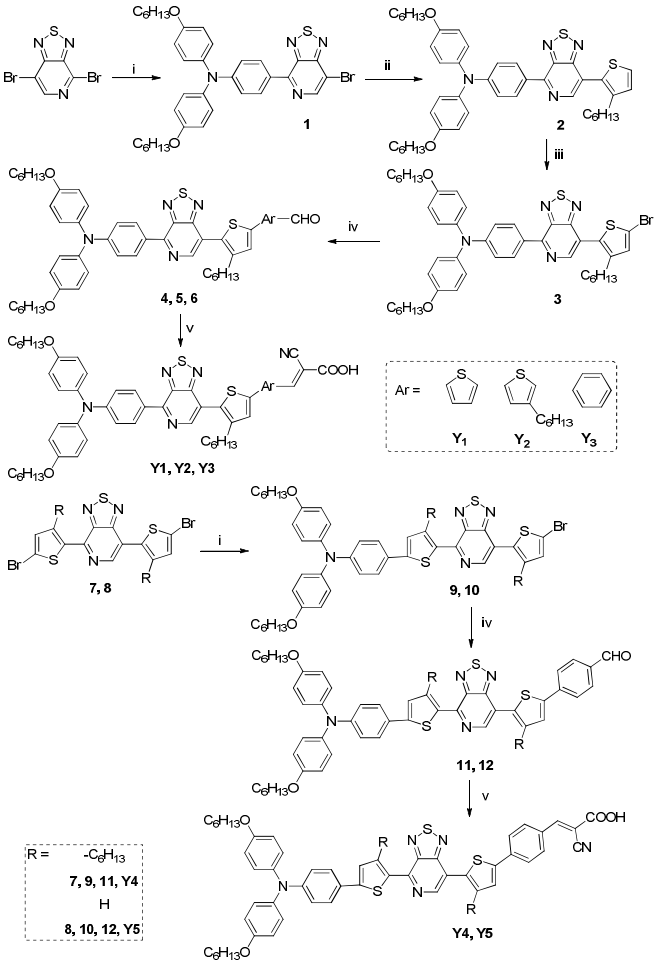

Scheme 1. Synthetic routes for **Y1-Y9**.

Photophysical Properties

The UV-vis absorption spectra of **Y1–Y5** in dichloromethane solutions are shown in **Figure 2** and the corresponding spectroscopic data are summarized in **Table 1**. They exhibit similar broad and strong absorption spectra covering a wide range of 300~800nm. The short wavelength peaks correspond to the π-π* transitions of the conjugated system and the long wavelength peaks can reasonably be assigned to the intramolecular charge transfer (ICT) from the donor to the acceptor. The absorption responses of **Y1–Y5** were effectively broadened due to the incorporation of the strong electron withdrawing thiadiazolo[3,4-*c*]pyridineunit in the π-conjugated spacer. As listed in **Table 1**, the absorption spectra of **Y1–Y3** display maximal absorption peaks at 554 nm with molar extinction coefficient (ε) of 1.78×10^4 M^{-1} cm^{-1}, 548 nm with ε of 1.89×10^4 $M^{-1}cm^{-1}$ and 540 nm with ε of 2.03×10^4 $M^{-1}cm^{-1}$, respectively. Notably, the maximal absorption peaks for the three sensitizers are blue-shifted in the order of **Y1** > **Y2** > **Y3**, indicating that the co-planarity of the molecules with different π-spacers decreases in the order of benzene > *n*-hexylthiophene > thiophene. On the other side, **Y4** and **Y5** show obviously red-shifted absorption peaks as well as higher molar extinction coefficients as compared with those of **Y1–Y3**, which can be attributed to the increased π-conjugation length by the incorporation of an additional *n*-hexylthiophene or thiophene in the π-spacer. The sensitizer **Y5** with two thiophene units adjacent to PyT instead of *n*-hexylthiophene in **Y4** exhibits larger bathochromic

shifts of the maximum absorption peaks and onset, which results from the good coplanar structure due to the less steric hindrance between the thiophene and PyT. When adsorbed on a transparent thin TiO_2 film, all sensitizers show slight hypsochromic shift of the absorption maxima and broad absorption spectra (**Figure 3**), which can be attributed probably to the formation of dye-dye aggregation or the deprotonation of the carboxylic acid when adsorbed on TiO_2 film. Notably, the shift is less pronounced for **Y4** on TiO_2 film relative to other sensitizers, which indicates that the intermolecular aggregation has been effectively suppressed because of the resistance of the long alkyl chains attached.

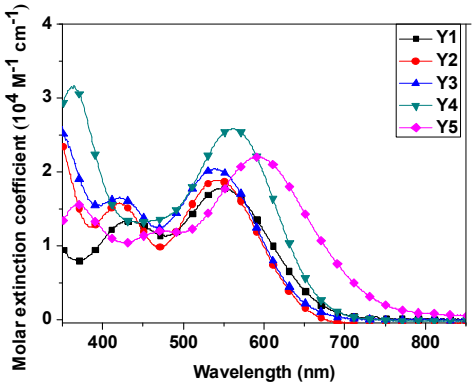

Figure 2. Absorption spectra of **Y1–Y5** in CH_2Cl_2 solutions.

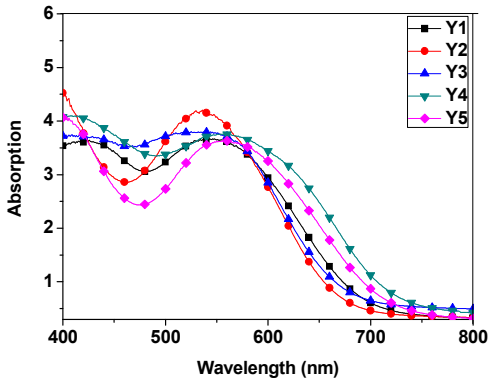

Figure 3. Absorption spectra of **Y1–Y5** on TiO_2 films.

Table 1. Absorption and electrochemical parameters for **Y1–Y5**.

Compd.	λ_{max} [a] ($\varepsilon/10^4$ $M^{-1}cm^{-1}$)/nm	λ_{max} [b]/nm	E_{ox} [c] /V	$E_{0\text{-}0}$ [d]/eV	E_{red} [e]/V
Y1	554 (1.78)	543	0.90	1.88	-0.98
Y2	548 (1.89)	539	0.87	1.90	-1.03
Y3	540 (2.03)	537	0.89	1.92	-1.03
Y4	563 (2.58)	561	0.86	1.86	-1.00
Y5	591 (2.21)	558	0.85	1.68	-0.83

[a] Absorption maximum in 1×10^{-5}mol L^{-1} CH_2Cl_2 solution. [b] Absorption maximum on TiO_2 film. [c] Oxidation potential in CH_2Cl_2 solution containing 0.1 M $(n\text{-}C_4H_9)_4NPF_6$ were calibrated with ferrocene (0.63 V *vs.* NHE) and taken as the HOMO. [d] $E_{0\text{-}0}$ was determined from the onset of absorption spectrum. [e] $E_{red} = E_{ox} - E_{0\text{-}0}$.

Electrochemical Properties

To evaluate the feasibility of electron injection and the possibility of dye regeneration, cyclic voltammograms have been recorded in CH_2Cl_2 solutions (**Figure 4**) to determine oxidation potentials (E_{ox}). The voltammograms for **Y1–Y5** show well symmetrical and reversible behaviors, indicative of high redox stability. Their HOMO and LUMO levels are summarized in **Table 1**. The HOMO levels of them are more positive than iodide/tri-iodide redox couples (~ 0.4 V), indicating that the oxidized dyes can be efficiently regenerated by the electrolyte. The zero-zero band gaps ($E_{0\text{-}0}$) estimated from the onset of the UV-visible absorption spectra, are in the range of 1.68–1.92 eV. Apparently, the incorporation of the strong electron-deficient PyT unit can effectively adjust the HOMO and LUMO levels, resulting in narrow energy band gaps and broad absorption spectra. Subsequently, the LUMO levels for **Y1–Y5**, as calculated from $E_{HOMO}-E_{0\text{-}0}$, are in the range of −1.03 to −0.83 V, sufficiently more negative than the conduction band edge energy level (E_{CB}) of TiO_2 semiconductor (−0.5 V vs. NHE), energetically allowing an efficient electron injection into the TiO_2 conduction band from the excited sensitizers. Therefore, the processes of electron injection and dye regeneration in DSSCs based on the sensitizers are feasible.

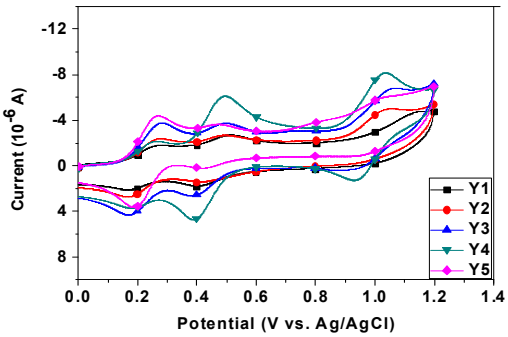

Figure 4. Oxidation potential of **Y1–Y5** in CH_2Cl_2 solutions.

Molecular Calculations

To gain insights into the geometrical and electronic properties of the five sensitizers, density functional calculations (DFT) were performed using the Gaussian 03 program package at the B3LYP/6-31G(d)*. As shown in **Figure 5**, the electron densities of LUMO orbitals of **Y1–Y5** are mainly delocalized across the entire π-conjugated spacer and the cyanoacrylic acid segment. And the HOMO orbitals of **Y1** and **Y2** are delocalized over the whole π-conjugation systems from the donor to the cyanoacrylic acid acceptor, while the HOMOs of **Y3**, **Y4** and**Y5** are primarily located at the donor groups and π-conjugated spacer, which were broken at the benzyl segment adjacent to the PyT core. For **Y1–Y5**, the dihedral angles formed between the π-conjugated spacer (PyT and *n*-hexylthiophene/thiophene) and the different π-linked spacers (thiophene, *n*-hexylthiophene and benzene) adjacent to the anchoring group, were computed to 5.6°, 9.3°, 37.8°, 38.2, and 36.3°, respectively. Obviously, the large steric conformation may interrupt the conjugation system and weaken the ICT interactions, resulting in a blue-shift of the maximum absorption band in the order of **Y3** < **Y2** < **Y1**, which is consistent with the experimental observation in the absorption spectra in solutions. In brief, the benzyl segment adjacent to PyT core in **Y3**, **Y4** and **Y5** led to a well segregated HOMO and LUMO orbitals without the exclusion of sufficient overlap between them, which guarantees a fast charge transfer transition from the donating group to the terminal acceptor, and

finally into the conduction band of TiO_2.

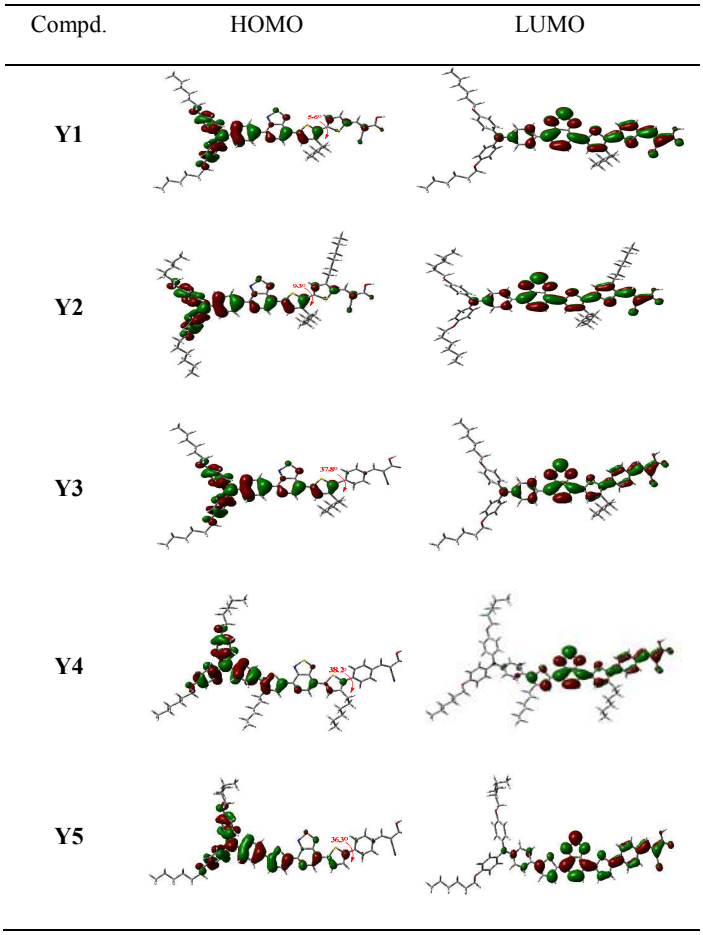

Figure 5. Calculated HOMO and LUMO profiles of **Y1–Y5**.

Photovoltaic Properties of DSSCs

Figure 6 shows the incident photon-to-current conversion efficiency (IPCE) curves of DSSCs based on the five sensitizers. Overall, the cells based on **Y1–Y5** exhibit remarkably broad IPCE action spectra covering the whole visible region and part of near-infrared (NIR) region. The IPCE value at around 560 nm for **Y3** (52%) is higher than that of **Y1** (31%) or **Y2** (46%). The IPCE as a function of wavelength is directly related to the light-harvesting efficiency (LHE), charge injection efficiency (Φ_{inj}) and charge collection efficiency (Φ_{col}).[3c] Disregarding the similar LUMO level and LHE values as well as the same anchoring group for the three sensitizers **Y1**–**Y3**, a higher IPCE value for **Y3** with phenyl group adjacent to PyT as π-conjugated spacer should be ascribed to the higher charge collection efficiency. Apparently, the charge collection efficiency follows the spacer order of benzene > *n*-hexylthiophene > thiophene. The result indicates that the introduction of the phenyl group instead of thiophene or *n*-hexylthiophene in the π-conjugated spacer has a positive effect on IPCE value. Impressively, **Y4** with a more extended π-conjugation network shows a much broader IPCE spectrum with the value at 560 nm above 60%. For comparison, **Y5** based device shows a little broader IPCE response than that of **Y4**, but the IPCE plateau decreases dramatically to around 20%. The most inferior IPCE value for **Y5** probably arises from the intermolecular π-stacked aggregation on TiO_2 surface due to the lack of long alkyl chains as well as its unsuitable LUMO level, which leads to a reduction in the yield of electron injection owing to intermolecular energy transfer.[15]

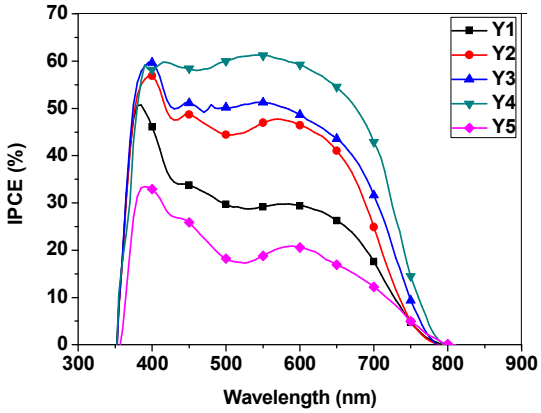

Figure 6. IPCE curves of DSSCs based on **Y1–Y5**.

The photocurrent-voltage (*J–V*) characteristics of liquid DSSCs based on **Y1–Y5** are shown in **Figure 7** and the photovoltaic parameters are collected in **Table 2**. The **Y1** and **Y2** sensitized solar cells give a short-circuit photocurrent (J_{sc}) of 6.47 and 8.42 mA cm^{-2}, an open-circuit photovoltage (V_{oc}) of 0.655 and 0.657 V, and a fill factor (*FF*) of 0.672 and 0.694, corresponding to an overall conversion efficiencies (η) of 2.89% and 3.84%, respectively. With a relatively higher J_{sc} and V_{oc}, DSSC based on **Y3** exhibits much higher conversion efficiency of 4.46%. The three sensitizers **Y1–Y3** have a similar chemical structure, but their photovoltaic performances exhibit much difference. The higher photocurrent and photovoltage of the device sensitized with **Y3** should be mainly attributed to the more efficient charge collection efficiency and less dye aggregation occurring on the TiO_2 film because of the decreased co-planarity of π-conjugation system, which was also supported by the DFT molecular calculation. The DSSC based on **Y4** shows the best photovoltaic performance with a J_{sc} of 12.45 mA cm^{-2}, a V_{oc} of 0.749 V, and a FF of 0.671, corresponding to the η value of 6.30%, which reaches 87% of the referenced **N719**-based DSSC (7.27%) fabricated under similar conditions. Though the efficiencies of DSSCs based on these dyes could not compete with that of N719 dye, the systematic study of structure-property relationships of these new dyes sheds light on optimizing D-A-π-A configuration metal-free organic dyes for highly efficient DSSCs. Among the five sensitizers, **Y4** shows the highest molar extinction coefficient and IPCE value in DSSC. In general, J_{sc} is related to the molar extinction coefficient of the sensitizer, in which a higher molar extinction coefficient correlates with good light-harvesting ability and a higher J_{sc} value. Moreover, the introduction of a twisted benzene spacer and the long alkyl chains in the π-conjugated bridge can interrupt the co-planarity of molecular dye and inhibit the back electron transfer, as a result, the dye aggregation and charge recombination rate can be slowed down in a large degree. All in all, it's not surprising that **Y4** gives the highest J_{sc} and V_{oc} values in this study. For comparison, the cell sensitized with the dye **Y5** without *n*-hexyl chains on the thiophene units shows the most inferior J_{sc} (3.24 mA cm^{-2}) and V_{oc} (0.650 V), leading to a significantly low η value of 1.32%, even though it shows much broader absorption spectral response above 800 nm in solution. Three DSSCs were also fabricated from the **Y5** containing the co-adsorbent chenodeoxycholic acid (CDCA) at different concentrations (0, 10 and 30 mM). An improved efficiency of DSSC based on **Y5** and 10 mM CDCA was improved to 2.11% (**Figure S1**). The inferior photocurrent for **Y5** should be attributed to

its good co-planarity of the π-conjugates spacer, which is liable to form intermolecular π-π stacked aggregation on the TiO_2 surface, leading to a significantly decrease in electron injection efficiency.[9a,15]

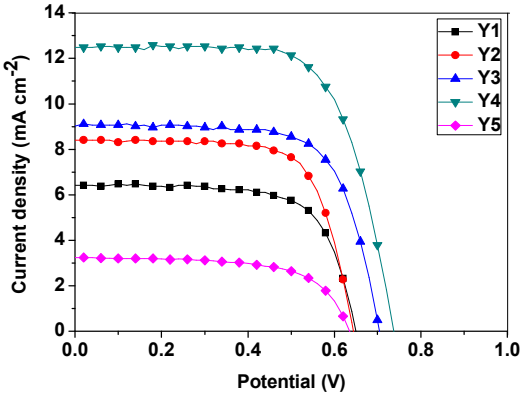

Figure 7. *J–V* curves of **Y1–Y5** sensitized solar cells.

Electrochemical Impedance Spectroscopy Analysis

Electrochemical Impedance Spectroscopy (EIS) analysis has been performed to elucidate the interfacial charge recombination process under a forward bias of −0.73 V in the dark (**Figure 8**). Some important parameters (R_s, R_{rec}, and R_{CE}) can be obtained by fitting the EIS curves using Z-view software (**Table 2**). In general, R_s, R_{rec}, and R_{CE} represent series resistance and charge transfer processes at the dye/TiO_2/electrolyte interface and counter electrode (CE), respectively.[16] The R_S and R_{CE} corresponding to the smaller semicircles show almost the same values in all the DSSCs due to their same electrode and electrolyte. And the R_{rec} corresponding to the larger semicircle, is related to the charge recombination rate between the TiO_2 film and the electrolyte, generally a smaller R_{rec} value indicates a faster charge recombination, thus giving a lower V_{oc}.[8e] The R_{rec} values for DSSCs based on these sensitizers increase in the order of **Y5** < **Y1** < **Y2** < **Y3** < **Y4**. The trend observed here are consistent with the results yielded for the V_{oc} values. Among the **Y1–Y3**, **Y3** sensitized DSSC shows the highest V_{oc} of 0.717 V, indicating that the twisted benzene unit in **Y3** could be more efficient for electron injection and back reaction suppression of the injected electron with I_3^- ion in the electrolyte. Moreover, *n*-hexylthiophene-bridged sensitizer **Y4** is more effective than the thiophene-bridged one **Y5** for blocking I_3^- ions approaching the TiO_2 surface, thus retarding the charge recombination between TiO_2 film and the electrolyte, resulting in the highest V_{oc} value (0.749 V) among the five sensitizers. It can be concluded that these dyes containing benzene unit as the π-linker and *n*-hexylthiophene unit as π-conjugation should be beneficial to the device performances.

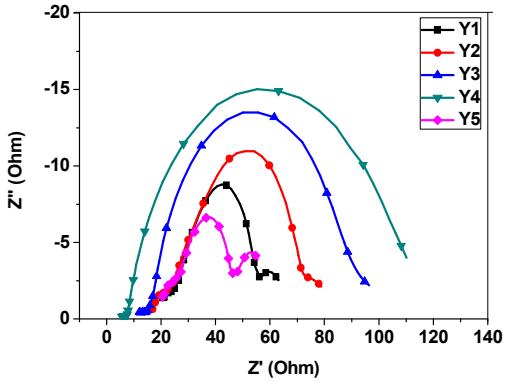

Figure 8. EIS Nyquist plots for DSSCs based on **Y1–Y5** under dark.

Table 2. Photovoltaic parameters of DSSCs under full sunlight illumination (AM 1.5G, 100 mW cm^{-2})[a]

Dye	J_{sc}/mA cm^{-2}	V_{oc}/V	FF	η/%	R_{rec}/Ωcm^{-1}
Y1	6.47	0.665	0.672	2.86	70.2
Y2	8.42	0.657	0.694	3.84	54.1
Y3	9.05	0.717	0.687	4.46	132.1
Y4	12.54	0.749	0.671	6.30	322.8
Y5	3.24	0.650	0.627	1.32	50.1
N719	14.39	0.742	0.680	7.27	/

[a] Performance of DSSCs measured in a 0.24 cm^2 working area on a FTO substrate at room temperature. Dyes were maintained at 0.5 mM in CH_2Cl_2 solution for **Yn** dyes. Electrolyte: LiI (0.05 M), I_2 (0.1 M), and DMPII (0.6 M) in acetonitrile:*tert*-butyl alcohol (1:1, v/v).

Conclusions

In summary, a series of thiadiazolo[3,4-*c*]pyridine-cored metal-free panchromatic organic sensitizers has been synthesized and applied in DSSC applications. It was demonstrated that the introduction of PyT unit in the π-conjugation frameworks could effectively tune the energy levels and produce a narrow band-gap sensitizer with panchromatic spectral response. For **Y1–Y3**, the dihedral angles formed between the π-conjugated spacer (PyT and *n*-hexylthiophene) and the different linkers (thiophene, *n*-hexylthiophene and benzene) adjacent to the anchoring group increase in the order **Y1** < **Y2** < **Y3**. As a result, **Y3** featuring the largest steric hindrance between the π-conjugated spacer and the phenyl linker produces higher photocurrent and photovoltage, which is attributed to the effective inhibition of intermolecular π-π stacked aggregation on the TiO_2 surface as well as the charge recombination. Impressively, the sensitizer **Y4** further optimized with a *n*-hexylthiophene inserted between the donor and PyT segment exhibits the best photovoltaic performance, mainly owing to the good light-harvesting property, the inhibition of π-π stacked dye aggregation on TiO_2 film, the efficient electron injection from the excited sensitizers, and the effectively retarded charge recombination by shielding the surface of TiO_2 from the I_3^- ions with long alkyl chains. For comparison, **Y5** with thiophene instead of *n*-hexylthiophene in **Y4** shows much broader absorption spectral response above 800 nm in solution, however, the most inferior photocurrent and photovoltage values should be attributed to its

highly co-planar π-conjugated spacer, which is liable to form intermolecular π-π stacked aggregation on the TiO_2 surface, leading to a low electron injection efficiency and quick charge recombination. The primary findings will facilitate the development of new metal-free PyT-cored organic dyes with panchromatic absorption for efficient DSSC applications.

Experimental Section

Materials. All solvents and reagents were purchased from Sigma-Aldrich Company and used as received without further purification. TiO_2 paste and iodide-based liquid electrolyte (HL-HPE) were purchased from Dyesol Ltd. The important intermediates of 4,7-dibromo-[1,2,5]thiadiazolo[3,4-*c*]pyridine,[13a] 4,7-bis(5-bromothiophen-2-yl)-[1,2,5]thiadiazolo[3,4-*c*]pyridine,[13a] 4,7-bis(5-bromo-3-hexylthiophen-2-yl)-[1,2,5]thiadiazolo[3,4-*c*]pyridine,[13a] and 4-(hexyloxy)-*N*-(4-(hexyloxy)phenyl)-*N*-(4-(4,4,5,5-tetramethyl-1,3,2-dioxaborolan-2-yl)phenyl)aniline[17] were synthesized according to the corresponding literature methods. The synthetic routs for **Y1–Y5** are outlined in Scheme 1 and the details are depicted as follows.

4-(7-Bromo-[1,2,5]thiadiazolo[3,4-*c*]pyridin-4-yl)-*N*,*N*-bis(4-(hexyloxy)phenyl)aniline (1)

The mixture of 4,7-dibromo-[1,2,5]thiadiazolo[3,4-*c*]pyridine (0.5 g, 1.7 mmol), 4-(hexyloxy)-*N*-(4-(hexyloxy)phenyl)-*N*-(4-(4,4,5,5-tetramethyl-1,3,2-dioxaborolan-2-yl)phenyl)aniline (1.0 g, 1.8 mmol), $Pd(PPh_3)_4$ (100 mg, 0.016 mmol) and 2 N aqueous solution of K_2CO_3 (2 mL) in THF (50 mL) under N_2 atmosphere was heated to reflux for 12 h. Then the solvent was removed under vacuum and the residue was purified by column chromatography on silica gel using a 1:4 mixture of hexane and CH_2Cl_2 as eluent to afford the red compound. Yield: 0.80 g, (72%). ^{1}H NMR (400 MHz, $CDCl_3$): δ (ppm) 8.69 (s, 1H), 8.42 (d, *J* = 6.4 Hz, 2H), 7.14 (t, *J* = 6.4 Hz, 2H), 6.99-7.06 (m, 4H), 6.80-6.88 (m, 4H), 3.95 (d, *J* = 6.4 Hz, 4H), 1.75-1.81 (m, 4H), 1.45-1.49 (m, 4H), 1.25-1.37 (m, 8H), 0.89 (t, *J* = 6.4 Hz, 6H).

4-(Hexyloxy)-*N*-(4-(hexyloxy)phenyl)-*N*-(4-(7-(3-hexylthiophen-2-yl)-[1,2,5]thiadiazolo[3,4-*c*]pyridin-4-yl)phenyl)aniline (2)

A mixture of **1** (0.80g, 1.14 mmol), tributyl(3-hexylthiophen-2-yl)stannane (0.69g, 1.5 mmol), $Pd(PPh_3)_4$ (100 mg, 0.016 mmol) in toluene (25 mL) was heated to reflux under a N_2 atmosphere for about 12 hrs. Then, the solvent was removed under vacuum and the residue was purified by column chromatography on silica gel using a 1:4 mixture of hexane and CH_2Cl_2 as eluent to afford the dark red compound. Yield: 0.82 g, (91%). ^{1}H NMR (400 MHz, $CDCl_3$): δ (ppm) 8.61 (s, 1H), 8.49 (d, *J* = 2.0 Hz, 1H), 7.83 (t, *J* = 2.0 Hz, 1H), 7.81 (t, *J* = 2.0 Hz, 1H), 7.15 (d, *J* = 2.0 Hz, 1H), 7.13 (t, *J* = 2.0 Hz, 2H), 7.10 (t, *J* = 2.0 Hz, 2H), 7.05 (t, *J* = 2.0 Hz, 1H), 7.03 (t, *J* = 2.0 Hz, 1H), 6.86 (t, J = 2.0 Hz, 2H), 6.83 (t, *J* = 2.0 Hz, 2H), 3.93 (t, J = 6.0 Hz, 4H), 2.72 (t, *J* = 7.2 Hz, 2H), 1.50-1.72 (m, 6H), 1.46-1.50 (m, 4H), 1.31-1.39 (m, 14H), 0.89-0.96 (m, 9H). ^{13}C NMR (400 MHz, $CDCl_3$): δ (ppm) 156.31, 155.94, 149.40, 148.30, 146.05, 145.15, 141.60, 141.50, 140.09, 132.77, 129.56, 127.21, 126.07, 125.64, 125.18, 119.53, 115.37, 68.27, 31.74, 31.66, 30.74, 30.51, 29.36, 29.07, 25.81, 22.91, 22.68, 14.18, 14.12. HRMS (MALDI-TOF, m/z): [M+] calcd for ($C_{45}H_{54}N_4O_2S_2$) 746.3746; found, 746.3749.

4-(7-(5-Bromo-3-hexylthiophen-2-yl)-[1,2,5]thiadiazolo[3,4-*c*]pyridin-4-yl)-*N*,*N*-bis(4 (hexyloxy)phenyl)aniline (3)

NBS (200 mg, 1.15 mmol) was added in one portion to the solution of **2** (0.8 g, 1.07 mmol) in THF (50 mL) at 0 °C. The mixture was allowed to warm to room temperature for overnight. Then, the reaction was quenched with water (50 mL), and extracted with dichloromethane. The collected organic layer was evaporated under vacuum and the residue was purified by column chromatography on silica gel with a 1:4 mixture of hexane and CH_2Cl_2 as eluent to afford the dark red compound. Yield: 0.88 g, (87%). ^{1}H NMR (400 MHz, $CDCl_3$): δ (ppm) 8.62 (s, 1H), 8.48 (d, *J* = 8.0 Hz, 1H), 7.84 (t, *J* = 8.0 Hz, 1H), 7.80 (t, J = 8.0 Hz, 1H), 7.16 (d, *J* = 8.0 Hz, 1H), 7.13 (t, *J* = 8.0 Hz, 2H), 7.10 (t, *J* = 8.0 Hz, 2H), 7.06 (t, *J* = 8.0 Hz, 1H), 7.02 (t, *J* = 8.0 Hz, 1H), 6.86 (t, *J* = 8.0 Hz, 2H), 6.83 (t, *J* = 8.0 Hz, 1H), 3.94 (t, *J* = 6.0 Hz, 4H), 2.73 (t, *J* = 7.2 Hz, 2H), 1.50-1.72 (m, 6H), 1.46-1.50 (m, 4H), 1.31-1.39 (m, 14H), 0.89-0.96 (m, 9H). ^{13}C NMR (400 MHz, $CDCl_3$): δ (ppm) 156.32, 155.92, 149.40, 148.30, 146.05, 145.15, 141.60, 141.50, 140.09, 132.77, 129.56, 127.21, 126.07, 125.64, 125.17, 119.52, 115.97, 68.27, 31.74, 31.66, 30.74, 30.51, 29.36, 29.07, 25.81, 22.91, 22.68, 14.18, 14.13. HRMS (MALDI-TOF, m/z): [M+] calcd for ($C_{45}H_{53}N_4O_2S_2$) 824.2865; found, 824.2877.

General synthetic procedures for compounds **4–6** and **9–12** are similar to that of **1.**

5'-(4-(4-(Bis(4-(hexyloxy)phenyl)amino)phenyl)-[1,2,5]thiadiazolo[3,4-*c*]pyridin-7-yl)-4'-hexyl-[2,2'-bithiophene]-5-carbaldehyde (4)

A purple compound. Yield: 0.18 g, (74%). ^{1}H NMR (400 MHz, $CDCl_3$): δ (ppm) 9.89 (s, 1H), 8.64 (s, 1H), 8.56 (s, 1H), 7.84 (d, *J* = 8.8 Hz, 2H), 7.69 (s, 1H), 7.12 (d, *J* = 8.8 Hz, 5H), 7.04 (d, *J* = 8.8 Hz, 2H), 6.85 (d, *J* = 8.8 Hz, 4H), 3.94 (t, *J* = 6.8 Hz, 4H), 2.94 (t, *J* = 6.8 Hz, 2H), 1.75-1.82 (m, 4H), 1.45-1.48 (m, 6H), 1.25-1.36 (m, 14H), 0.87-0.92 (m, 9H). ^{13}C NMR (400 MHz, $CDCl_3$): δ (ppm) 182.88, 156.32, 156.02, 149.58, 148.35, 145.26, 144.91, 143.95, 142.74, 142.27, 141.55, 139.99, 139.45, 137.70, 133.01, 132.05, 129.63, 127.26, 126.61, 125.40, 119.42, 115.40, 68.29, 31.63, 31.59, 30.72, 29.33, 27.87, 25.79, 22.65, 22.61, 17.55, 14.08, 14.11. HRMS (MALDI-TOF, m/z): [M+] calcd for ($C_{50}H_{56}N_4O_3S_3$) 856.3547; found, 856.3543.

5'-(4-(4-(Bis(4-(hexyloxy)phenyl)amino)phenyl)-[1,2,5]thiadiazolo[3,4-*c*]pyridin-7-yl)-4,4'-dihexyl-[2,2'-bithiophene]-5-carbaldehyde (5)

A purple compound. Yield: 0.17 g, (70%). ^{1}H NMR (400 MHz, CDCl3): δ (ppm) 9.91 (s, 1H), 8.64 (s, 1H), 8.52 (s, 1H), 7.83 (d, *J* = 7.2 Hz, 2H), 7.74 (d, *J* = 7.2 Hz, 1H), 7.38 (d, J = 4.0 Hz, 1H), 7.12-7.14 (m 4H), 7.03 (d, *J* = 8.0 Hz, 2H), 6.85-6.88 (m, 3H), 3.94 (t, *J* = 6.0 Hz, 4H), 2.90-2.94 (m, 4H), 1.75-1.82 (m, 4H), 1.43-1.47 (m, 4H), 1.29-1.36 (m, 14H), 0.87-0.92 (m, 12H). 13C NMR (400 MHz, CDCl3): δ (ppm) 182.71, 156.31, 156.01, 149.54, 148.36, 145.42, 142.06, 141.58, 141.13, 141.05, 140.72, 140.01, 135.05, 134.51, 130.06, 129.76, 129.61, 127.29, 126.75, 125.46, 119.34, 115.38, 68.28, 31.71, 31.65, 31.61, 30.85, 30.27, 30.15, 29.73, 29.34, 27.88, 26.89, 25.80, 22.67, 22.63, 17.56, 14.16, 14.11, 13.67. HRMS (MALDI-TOF, m/z): [M+] calcd for (C56H68N4O3S3) 940.4517;

found, 940.4523.

4-(5-(4-(4-(Bis(4-(hexyloxy)phenyl)amino)phenyl)-[1,2,5]thiadiazolo[3,4-*c*]pyridin-7-yl)-4-hexylthiophen-2-yl)benzaldehyde (6)

A purple compound. Yield: 0.21 g, (73%). ^{1}H NMR (400 MHz, $CDCl_3$): δ (ppm) 10.06 (s, 1H), 8.64 (s, 1H), 8.55 (s, 1H), 7.94-7.97 (m, 2H), 7.82-7.85 (m, 2H), 7.70 (d, *J* = 8.4 Hz, 2H), 7.10-7.14 (m, 4H), 7.03-7.07 (m, 2H), 6.85-6.89 (m, 4H), 3.94 (t, *J* = 6.0 Hz, 4H), 2.93 (t, *J* = 7.2 Hz, 2H), 1.61-1.78 (m, 6H), 1.36-1.49 (m, 4H), 1.27-1.35 (m, 14H), 0.85-0.93 (m, 9H). ^{13}C NMR (400 MHz, $CDCl_3$): δ (ppm) 191.64, 156.31, 156.01, 149.54, 148.36, 145.42, 142.06, 141.58, 141.05, 140.95, 140.72, 140.01, 135.29, 134.08, 130.06, 129.60, 129.54, 127.26, 126.47, 125.46, 119.43, 115.40, 68.29, 31.63, 31.61, 30.85, 29.73, 29.34, 29.27, 25.79, 22.65, 22.63, 14.09, 14.08. HRMS (MALDI-TOF, m/z): [M+] calcd for ($C_{52}H_{58}N_4O_3S_2$) 850.4013; found, 850.4022.

4-(5-(7-(5-Bromo-3-hexylthiophen-2-yl)-[1,2,5]thiadiazolo[3,4-c]pyridin-4-yl)-4-hexylthiophen-2-yl)-*N*,*N*-bis(4-(hexyloxy)phenyl)aniline (9)

A dark red compound. Yield: 0.67 g, (76%). ^{1}H NMR (400 MHz, $CDCl_3$): δ (ppm) 8.63 (s, 1H), 8.54 (t, *J* = 4.0 Hz, 2H), 7.76 (d, *J* = 4.0 Hz, 1H), 7.43-7.48 (m, 2H), 7.05-7.16 (m, 4H), 6.97 (s, 1H), 6.90 (s, 1H), 6.86-6.89 (m, 4H), 3.94 (t, *J* = 7.2 Hz, 4H), 1.76-1.80 (m, 4H), 1.47-1.56 (m, 4H), 1.33-1.38 (m, 8H), 0.93 (t, *J* = 7.6 Hz, 6H). ^{13}C NMR (400 MHz, $CDCl_3$): δ (ppm) 155.90, 154.52, 150.33, 149.21, 147.83, 146.49, 140.47, 140.01, 138.98, 138.29, 133.74, 130.80, 127.23, 127.06, 126.65, 125.24, 123.44, 119.63, 118.78, 115.34, 114.45, 68.26, 31.74, 31.65, 31.66, 30.99, 30.83, 29.45, 29.34, 29.25, 29.16, 25.86, 25.03, 22.65, 22.66, 22.46, 14.15, 14.12, 14.10 HRMS (MALDI-TOF, m/z): [M^+] calcd for ($C_{55}H_{67}BrN_4O_2S_3$) 990.3648; found, 990.3643.

4-(5-(7-(5-Bromothiophen-2-yl)-[1,2,5]thiadiazolo[3,4-*c*]pyridin-4-yl)thiophen-2-yl)-N,N-bis(4-(hexyloxy)phenyl)aniline (10)

A dark red compound. Yield: 0.89 g, (78%). ^{1}H NMR (400 MHz, $CDCl_3$): δ (ppm) δ (ppm) 8.65 (s, 1H), 8.53 (t, *J* = 4.0 Hz, 2H), 7.72 (d, *J* = 4.0 Hz, 1H), 7.47-7.49 (m, 2H), 7.06-7.11 (m, 4H), 6.92 (s, 1H), 6.90 (s, 1H), 6.86-6.89 (m, 4H), 3.94 (t, *J* = 7.2 Hz, 4H), 1.75-1.80 (m, 4H), 1.43-1.49 (m, 4H), 1.33-1.37 (m, 8H), 0.90 (t, *J* = 7.6 Hz, 6H). ^{13}C NMR (400 MHz, $CDCl_3$): δ (ppm) 155.90, 154.51, 150.13, 149.22, 147.89, 146.49, 140.47, 140.00, 138.95, 138.29, 133.74, 130.80, 127.20, 127.06, 126.65, 125.20, 123.44, 119.63, 118.77, 115.34, 114.43, 68.27, 31.66, 29.36, 25.82, 22.68, 14.12. HRMS (MALDI-TOF, m/z): [M+] calcd for ($C_{43}H_{43}BrN_4O_2S_3$) 822.1747; found, 822.1741.

4-(5-(4-(5-(4-(Bis(4-(hexyloxy)phenyl)amino)phenyl)-3-hexylthiophen-2-yl)-[1,2,5]thiadiazolo[3,4-*c*]pyridin-7-yl)-4-hexylthiophen-2-yl)benzaldehyde (11)

A purple red compound. Yield: 0.24 g, (81%). ^{1}H NMR (400 MHz, $CDCl_3$): δ (ppm) 10.05 (s, 1H), 8.77 (s, 1H), 8.51 (s, 1H), 7.93-7.97 (m, 3H), 7.67 (d, *J* = 8.4 Hz, 2H), 7.32-7.34 (m, 2H), 7.09-7.13 (m, 4H), 6.94 (t, *J* = 8.8 Hz, 2H), 6.85-6.89 (m, 4H), 3.94 (t, *J* = 6.8 Hz, 4H), 2.72-2.78 (m, 4H), 1.62-1.78 (m, 6H), 1.40-1.48 (m, 4H), 1.27-1.38 (m, 22H), 0.89-0.93 (m, 12H). ^{13}C NMR (400 MHz, $CDCl_3$): δ (ppm) 191.68, 155.86, 154.82, 148.71, 148.11, 146.55, 144.72, 141.44, 140.90, 140.63, 140.17, 140.08, 138.05, 137.85, 136.30, 135.08, 131.78, 131.09, 130.52, 130.06, 129.57, 129.49, 127.13, 125.46, 119.28, 115.35, 68.26, 31.72, 31.63, 31.62, 30.99, 30.89, 29.35, 29.32, 29.24, 29.14, 25.80, 25.07, 22.69, 22.66, 22.45, 14.17, 14.12, 14.10. HRMS (MALDI-TOF, m/z): [M+] calcd for ($C_{62}H_{72}N_4O_3S_3$) 1016.4845; found, 1016.4841.

4-(5-(4-(5-(4-(Bis(4-(hexyloxy)phenyl)amino)phenyl)thiophen-2-yl)-[1,2,5]thiadiazolo[3,4-*c*]pyridin-7-yl)thiophen-2-yl)benzaldehyde (12)

A purple compound. Yield: 0.16 g, (74%). ^{1}H NMR (400 MHz, $CDCl_3$): δ (ppm) 9.95 (s, 1H), 8.72 (s, 1H), 8.50 (d, *J* = 7.2 Hz, 1H), 7.96-8.00 (m, 6H), 7.85 (d, *J* = 7.2 Hz, 2H), 7.73-7.79 (m, 2H), 7.43-7.48 (m, 4H), 7.23 (d, *J* = 8.8 Hz, 1H), 7.07-7.09 (m, 2H), 6.84-6.87 (m, 2H), 3.94 (t, *J* = 7.2 Hz, 4H), 2.67-2.78 (m, 4H), 1.75-1.80 (m, 4H), 1.45-1.49 (m, 4H), 1.33-1.37 (m, 8H), 0.93 (d, *J* = 8.8 Hz, 6H). ^{13}C NMR (400 MHz, $CDCl_3$): δ (ppm) 182.53, 155.89, 154.34, 148.65, 147.83, 146.33, 145.93, 144.90, 142.91, 142.23, 140.33, 140.14, 139.97, 137.88, 136.78, 136.54, 130.92, 130.47, 129.45, 127.15, 126.92, 126.04, 125.41, 119.23, 118.50, 115.36, 68.28, 31.67, 29.38, 25.86, 22.69, 14.10. HRMS (MALDI-TOF, m/z): [M+] calcd for ($C_{50}H_{48}N_4O_3S_3$) 848.2901; found, 848.2917.

General synthetic procedures for the preparation of sensitizers **Y1–Y5.**

A mixture of the precursor carbaldehyde (0.20 mmol) and cyanoacyclic acid (100 mg, 1.30 mmol) in acetic acid (20 mL) was refluxed in the presence of ammonium acetate (200 mg) overnight under a N_2 atmosphere. Then, water was added and extracted with CH_2Cl_2. Next, the solvent was removed under vacuum and the crude compound was purified by column chromatography on silica gel eluting with CH_2Cl_2/MeOH (20:1, v/v) to give targeted dyes.

(*E*)-3-(5'-(4-(4-(Bis(4-(hexyloxy)phenyl)amino)phenyl)-[1,2,5]thiadiazolo[3,4-*c*]pyridin-7-yl)-4'-hexyl-[2,2'-bithiophen]-5-yl)-2-cyanoacrylic acid (Y1)

A dark purple compound. Yield: 0.10 g, (70%). ^{1}H NMR (400 MHz, $CDCl_3$ + DMSO-d_6): δ (ppm) 8.55 (s, 1H), 8.29 (s, 1H), 8.15 (s, 1H), 7.81 (d, *J* = 8.8 Hz, 2H), 7.75 (s, 1H), 7.38 (d, *J* = 4.0 Hz, 1H), 6.99 (d, *J* = 8.8 Hz, 4H), 6.86 (d, *J* = 8.8 Hz, 4H), 6.76 (d, *J* = 8.8 Hz, 2H), 3.90 (t, *J* = 6.4 Hz, 4H), 2.77 (t, *J* = 7.2 Hz, 2H), 1.58-1.70 (m, 6H), 1.27-1.38 (m, 6H), 1.16-1.20 (m, 12H), 0.82-0.87 (m, 9H). ^{13}C NMR (400 MHz, $CDCl_3$ + DMSO-d_6): δ (ppm) 155.43, 155.36, 148.75, 147.45, 144.24, 141.17, 140.74, 140.34, 139.25, 137.44, 136.02, 135.63, 133.54, 131.27, 130.52, 129.24, 128.78, 126.86, 125.42, 124.79, 118.37, 116.97, 115.12, 113.50, 113.05, 67.58, 31.05, 30.21, 29.03, 28.75, 28.62, 25.23, 25.15, 24.57, 22.09, 13.79, 13.78. HRMS (MALDI-TOF, m/z): [M^+] calcd for ($C_{53}H_{57}N_5O_4S_3$) 924.4017; found, 924.3999.

(*E*)-3-(5'-(4-(4-(Bis(4-(hexyloxy)phenyl)amino)phenyl)-[1,2,5]thiadiazolo[3,4-*c*]pyridin-7-yl)-4,4'-dihexyl-[2,2'-bithiophen]-5-yl)-2-cyanoacrylic acid (Y2)

A dark purple compound. Yield: 0.11 g, (71%). ^{1}H NMR (400 MHz, $CDCl_3$ + DMSO-d_6): δ (ppm) 8.59 (s, 1H), 8.49 (s, 1H), 8.17 (s, 1H), 7.83 (d, *J* = 8.4 Hz, 2H), 7.68 (s, 1H), 7.02 (d, *J* = 8.4 Hz, 4H), 6.82-6.87 (m, 6H), 3.88 (t, *J* = 6.4 Hz, 4H), 2.55-2.63 (m, 4H),

1.60-1.70 (m, 4H), 1.52-1.58 (m, 6H), 1.36-1.41 (m, 4H), 1.24-1.31 (m, 18H), 0.79-0.86 (m, 12H). ^{13}C NMR (400 MHz, $CDCl_3$ + DMSO-$_{d6}$): δ (ppm) 155.53, 154.33, 148.92, 147.54, 144.18, 144.01, 142.86, 141.82, 141.27, 140.81, 139.26, 136.00, 135.69, 132.50, 131.46, 129.42, 128.70, 126.93, 125.78, 124.82, 122.21, 118.42, 117.25, 115.21, 112.15, 67.59, 31.03, 30.98, 30.97, 30.13, 29.86, 28.73, 28.43, 28.36, 27.65, 26.44, 25.22, 22.09, 21.98, 13.80, 13.77, 13.57. HRMS (MALDI-TOF, m/z): [M$^+$] calcd for ($C_{59}H_{69}N_5O_4S_3$) 1009.4812; found, 1009.4832.

(*E*)-3-(4-(5-(4-(4-(bis(4-(hexyloxy)phenyl)amino)phenyl)-[1,2,5]thiadiazolo[3,4-*c*]pyridin-7-yl)-4-hexylthiophen-2-yl)phenyl)-2-cyanoacrylic acid (Y3)

A dark purple compound. Yield: 0.12 g, (69%). ^{1}H NMR (400 MHz, $CDCl_3$ + DMSO-d_6): δ (ppm) 8.51 (s, 1H), 8.39 (s, 1H), 8.12 (s, 1H), 7.84 (d, *J* = 1.6 Hz, 2H), 7.77 (t, J = 6.8 Hz, 2H), 7.61 (s, 1H), 7.26 (d, *J* = 3.6 Hz, 1H), 7.02 (d, *J* = 9.2 Hz, 4H), 6.86 (d, *J* = 8.8 Hz, 2H), 6.77 (d, *J* = 8.8 Hz, 4H), 3.86 (t, *J* = 6.4 Hz, 4H), 2.81 (t, *J* = 7.6 Hz, 2H), 1.64-1.71 (m, 6H), 1.35-1.41 (m, 6H), 1.16-1.27 (m, 12H), 0.79-0.84 (m, 9H). ^{13}C NMR (400 MHz, $CDCl_3$ + DMSO-d_6): δ (ppm) 167.65, 157.60, 155.55, 148.87, 147.48, 143.33, 142.08, 141.14, 140.84, 140.15, 139.25, 137.95, 137.07, 136.17, 135.94, 133.86, 133.72, 133.27, 129.45, 127.00, 126.51, 125.64, 124.79, 118.33, 115.28, 67.59, 31.07, 31.04, 29.82, 29.52, 29.43, 28.74, 28.66, 25.23, 22.10, 13.88, 13.85. HRMS (MALDI-TOF, m/z): [M$^+$] calcd for ($C_{55}H_{59}N_5O_4S_2$) 918.5082; found, 918.5096.

(E)-3-(4-(5-(4-(5-(4-(bis(4-(hexyloxy)phenyl)amino)phenyl)-3-hexylthiophen-2-yl)-[1,2,5]thiadiazolo[3,4-*c*]pyridin-7-yl)-4-hexylthiophen-2-yl)phenyl)-2-cyanoacrylic acid (Y4)

A purple compound. Yield: 0.14 g, (77%). ^{1}H NMR (400 MHz, $CDCl_3$ + DMSO-d_6): δ (ppm) 8.59 (s, 1H), 8.17-8.22 (m, 2H), 8.02 (d, *J* = 8.0 Hz, 2H), 7.83 (s, 1H), 7.50 (d, *J* = 8.0 Hz, 2H), 7.13 (d, *J* = 8.4 Hz, 2H), 6.94 (d, *J* = 8.4 Hz, 4H), 6.79 (d, *J* = 8.4 Hz, 4H), 6.71 (d, *J* = 8.4 Hz, 2H), 3.86 (t, *J* = 2.0 Hz, 4H), 2.60 (t, *J* = 6.0 Hz, 4H), 1.63-1.70 (m, 5H), 1.36-1.39 (m, 5H), 1.21-1.28 (m, 22H), 0.79-0.86 (m, 12H). ^{13}C NMR (400 MHz, $CDCl_3$ + DMSO-d_6): δ (ppm) 163.76, 155.96, 154.10, 152.70, 148.63, 147.43, 145.35, 143.77, 141.18, 140.43, 139.78, 139.42, 138.37, 138.15, 137.84, 135.83, 134.45, 131.37, 130.95, 130.48, 129.45, 129.05, 127.43, 124.97, 118.93, 118.68, 116.80, 115.73, 68.06, 31.53, 31.27, 31.03, 30.73, 30.56, 30.24, 29.23, 29.12, 29.03, 26.24, 25.73, 24.71, 24.03, 22.59, 14.37, 14.34. HRMS (MALDI-TOF, m/z): [M+] calcd for ($C_{65}H_{73}N_5O_4S_3$) 1084.4903; found, 1084.4940.

(E)-3-(4-(5-(4-(5-(4-(bis(4-(hexyloxy)phenyl)amino)phenyl)-thiophen-2-yl)-[1,2,5]thiadiazolo[3,4-*c*]pyridin-7-yl)thiophen-2-yl)phenyl)-2-cyanoacrylic acid (Y5)

A dark compound. Yield: 0.13 g, (67%). ^{1}H NMR (400 MHz, $CDCl_3$ + DMSO-d_6): δ (ppm) 8.70 (s, 1H), 8.32 (s, 1H), 8.28 (s, 1H), 7.95 (s, 1H), 7.76 (s, 1H), 7.20 (d, *J* = 8.0 Hz, 2H), 6.97 (d, *J* = 8.0 Hz, 4H), 6.75-6.80 (m, 6H), 3.86 (t, *J* = 6.0 Hz, 4H), 2.48-2.59 (m, 6H), 1.62-1.70 (m, 5H), 1.54-1.58 (m, 8H), 1.32-1.39 (m, 5H), 1.19-1.28 (m, 22H), 0.84-1.09 (m, 15H). ^{13}C NMR (400 MHz, $CDCl_3$ + DMSO-d_6): δ (ppm) 163.63, 155.47, 153.83, 150.69, 149.70, 148.24, 147.08, 145.33, 144.94, 144.65, 143.58, 143.41, 142.84, 140.41, 139.29, 139.15, 137.67, 136.64, 135.50, 134.31, 132.15, 129.01, 128.51, 126.90, 124.46, 118.42, 118.25, 116.53, 115.18, 67.57, 31.06, 31.04, 31.00, 30.90, 30.36, 30.31, 30.11, 29.85, 29.05, 28.74, 28.66, 28.53, 28.39, 28.19, 27.63, 26.42, 25.23, 22.09, 22.04, 22.00, 13.85, 13.81, 13.56. HRMS (MALDI-TOF, m/z): [M+] calcd for ($C_{69}H_{83}N_5O_4S_4$) 1174.5406; found, 1174.5401.

Measurement and Characterizations. ^{1}H and ^{13}C NMR spectra were recorded with a Bruker Ultrashield 400 Plus NMR spectrometer. The UV-visible absorption spectra of these dyes were measured in CH_2Cl_2 solutions with a Varian Cary 100 UV-Vis spectrophotometer. Emission spectra were performed using a Photon Technology International (PTI) Alpha scan spectrofluorimeter. High-resolution matrix-assisted laser desorption/ionization time of flight (MALDI-TOF) mass spectra were obtained with a Bruker Autoflex MALDI-TOF mass spectrometer. The cyclic voltammograms (CV) were measured with Versastat II electrochemical work station using a normal three-electrode cell with a Pt working electrode, a Pt wire counter electrode and a Ag/Ag$^+$ reference electrode. The supporting electrolyte was 0.1 M *tetra*-n-butylammoniumhexafluorophosphate in DCM solution. The potential of the reference electrode was calibrated by ferrocene after each set of measurements, and all potentials mentioned in the work were against normal hydrogen electrode.

Cell Fabrication and characterization. To make a reasonable comparison, all the anode films for the DSSCs were made under the same standard manner, which are composed of 12 μm thick of transparent layer (TiO_2 with diameter of 20 nm) and 6 μm thick of scattering layer (TiO_2 nanoparticles with diameter of 200 nm). In specific, a doctor-blade technique was utilized to prepare photoanode (TiO_2) films. Firstly, a layer of ca. 6 μm TiO_2 paste (20 nm) was doctor-bladed onto the FTO conducting glass and then relaxed at room temperature for 3 min before heating at 150 °C for 6 min, this procedure was repeated once to achieve a film thickness of ca. 12 μm and the resulting surface was finally coated by a scattering layer (ca. 6 μm) of TiO_2 paste (200 nm). The electrodes were gradually heated under an air flow at 275 °C for 5 min, 325 °C for 5 min, 375 °C for 5 min, 470 °C for 30 min to remove polymers and generate three-dimensional TiO2 nanoparticle network. After that, the sintered films were soaked with 0.02 M TiF_4 aqueous solution for 45 min at 70°C, washed with deionized water, and further annealed at 450 °C for 30 min. After cooling down to ca. 80°C, the electrodes were immersed into a 5×10^{-4} M dye bath in CH_2Cl_2 solution for **Y1-Y5** dye series maintained in the dark for 16 hrs. Afterwards, the electrodes were rinsed with ethanol to remove the non-adsorbed dyes and dried in air. Pt counter electrodes were prepared by sputtering method at 15 mA for 90 s at a power of 150 W. Two holes (0.75 mm in diameter) were pre-drilled in the FTO glass for introducing electrolyte. The dye-adsorbed TiO_2 electrode and Pt-counter electrode were assembled into a sandwich type cell and sealed with a hot-melt parafilm at about 100 °C. The liquid electrolyte consisting of 0.6 M 1,2-dimethyl-3-propylimidazolium iodide (DMPII), 0.1 M LiI, 0.05 M I_2 in a mixture of acetonitrile and *tert*-butyl alcohol (volume ratio, 1:1) was introduced into the cell through the drilled holes at the back of the counter electrode. At last, the holes were sealed by parafilm and covering glass (0.1 mm thickness) at elevated temperature. The effective areas of all the TiO_2 electrodes were 0.24 cm^2. The current-voltage (*J-V*) characteristics of the assembled DSSCs were measured by a semiconductor characterization system (Keithley 236) at room

temperature in air under the spectral output from solar simulator (Newport) using an AM 1.5G filter with a light power of 100 mW/cm^2. IPCEs of DSSCs were recorded in Solar Cell QE/IPCE Measurement System (Zolix Solar Cell Scan 100) using DC mode. CHI 660D electrochemical workstation was used to characterize the electrochemical properties of the DSSCs. Electrochemical impedance spectroscopy (EIS) was recorded under dark condition over a frequency range of 0.1-105 Hz with an AC amplitude of 10 mV and the parameters were calculated from Z-View software (v2.1b, Scribner AssociatNe, Inc.).

Acknowledgments

We thank the National Natural Science Foundation of China (NSFC) (Grant 91222201), the Science, Technology and Innovation Committee of Shenzhen Municipality (JCYJ20120829154440583), Hong Kong Research Grants Council (HKBU203112, HKBU202811 and HKBU203011) and Hong Kong Baptist University (FRG2/12-13/083, FRG2/11-12/007) for the financial support. W.-K.W. and W.-Y.W. also thank a grant from Areas of Excellence cheme, University Grants Committee, Hong Kong (Project No. [AoE/P-03/08]). X. D. X and T. C acknowledge the financial support from the CUHK Group Research Scheme and CUHK Focused Scheme B Grant ''Center for Solar Energy Research''.

Notes and references

[a] *Institute of Molecular Functional Materials, Department of Chemistry and Institute of Advanced Materials, Hong Kong Baptist University, Waterloo Road, Kowloon Tong, Hong Kong, P. R. China. Fax: 85234117048; Tel: 85234115157; E-mail: xjzhu@hkbu.edu.hk; wkwong@hkbu.edu.hk; rwywong@hkbu.edu.hk.*
[b] *Department of Physics, the Chinese University of Hong Kong, Shatin, New Territories, Hong Kong, P. R. China. Fax: 85226035204; Tel: 85239436278; E-mail: taochen@phy.cuhk.edu.hk*
[c] *State Key Laboratory of Fine Chemicals, School of Chemical Engineering, Dalian University of Technology, Dalian, 116024, P. R. China.*
[d] *Photovotaic Materials Unit National Institute for Materials Science Sengen 1-2-1, Tsukuba, Ibaraki (Japan). Fax: (+81) 29-859-2304 E-mail: roverqin@gmail.com*
[§] *Y.H. and J.H. contribute equally to this work.*

1 B. O'Regan and M. Grätzel, *Nature*, 1991, **353**, 737.
2 a) M. K. Nazeeruddin, A. Kay, I. Rodicio, R. Humphry-Baker, E. Mueller, P. Liska, N. Vlachopoulos and M. Grätzel, *J. Am. Chem. Soc*, 1993, **115**, 8; b) M. Grätzel, *Inorg. Chem.*, 2005, **44**, 6841.
3 a) M. Nazeeruddin, F. De Angelis, S. Fantacci, A. Selloni, G. Viscardi, S. P. Liska, B. T. Ito and M. Grätzel, *J. Am. Chem. Soc*, 2005, **127**, 16835; b) M. K. Nazeeruddin, R. Splivallo, P. Liska, P. Comte and M. Grätzel, *Chem. Commun.*, 2003, 1456; c) A. Hagfeldt, G. Boschloo, L. Sun, L. Kloo and H. Pettersson, *Chem. Rev.*, 2010, **110**, 6595.
4. a) M. K. Nazeeruddin, P. Péchy and M. Grätzel, *Chem. Commun.*, 1997, **18**, 1705; b) M. K. Nazeeruddin, P. Pechy, T. Renouard, S. M. Zakeeruddin, R. Humphry-Baker, P. Comte, P. Liska, L. Cevey, E. Costa, V. Shklover, L. Spiccia, G. B. Deacon, C. A. Bignozzi and M. Grätzel, *J. Am. Chem. Soc.*, 2001, **123**, 1613; c) Y. Chiba, A. Islam, Y. Watanabe, R. Komiya, N. Koide and L. Han, *Jpn. J. Appl. Phys.*, 2006, **45**, L638; d) C. Y. Chen, M. K. Wang, J. Y. Li, N. Pootrakulchote, L. Alibabaei, C. H. Ngoc-le, J. D. Decoppet, J. H. Tsai, C. Grätzel, C. G. Wu, S. M. Zakeeruddin and M. Grätzel, *ACS Nano*, 2009, **3**, 3103; e) M. Kimura, J. Masuo, Y. Tohata, K. Obuchi, N. Masaki, T. N. Murakami, N. Koumura, K. Hara, A. Fukui, R. Yamanaka and S. Mori, *Chem. Eur. J.*, 2013, **19**, 1028; f) Q. Yu, Y. Wang, Z. Yi, N. Zu, J. Zhang, M. Zhang and P. Wang, *ACS Nano*, 2010, **4**, 6032–6038; g) L. Y. Han, A. Islam, H. Chen, C. Malapaka, B. Chiranjeevi, S. F. Zhang, X. D. Yang and M. Yanagida, *Energy Environ. Sci.*, 2012, **5**, 6057. h) H. Choi, M. Shin, K. Song, M. S. Kang, Y. Kang, J. Ko, *J. Mater. Chem. A*, 2014, **2**, 12931.
5 a) N. Koumura, Z.S. Wang, S. Mori, M. Miyashita, E. Suzuki and K. Hara, *J. Am. Chem. Soc.*, 2006, **128**, 14256; b) Y. M. Cao, Y. Bai, Q. J. Yu, Y. M. Cheng, S. Liu, D. Shi, F. Gao and P. Wang, *J. Phys. Chem. C*, 2009, **113**, 6290; c) J. Tang, W. J. Wu, J. L. Hua, J. Li, X. Li and H. Tian, *Energy Environ. Sci.*, 2009, **2**, 982; d) K. Pei, Y. Z. Wu, W. J. Wu, Q. Zhang, B. Q. Chen, H. Tian and W. H. Zhu, *Chem. Eur. J.*, 2012, **18**, 8190. c) Y. Hua, S. Chang, J, He.; C. S. Zhang, J. Z. Zhao, T. Chen, W. Y. Wong, W. K.Wong, X. J. Zhu, *Chem. Eur. J.*, 2014, **20**, 6300. d) B. Liu, B.Wang, R. Wang, L. Gao, S. H. Huo, Q. B. Liu, X. Y. Li, W. H. Zhu, *J. Mater. Chem. A*, 2014, **2**, 804.
6 a) C. Teng, X. C. Yang, S. F. Li, M. Cheng, A. Hagfeldt, L. Z. Wu, L. and C. Sun, *Chem. Eur. J.*, 2010, **16**, 13127; b) Y. Cui, Y. Z. Wu, X. F. Lu, X. Zhang, G. Zhou, F. B. Miapeh, W. H. Zhu and Z. S. Wang, *Chem. Mater.*, 2011, **23**, 4394; c) Y. C. Chen, Y. H. Chen, H. H. Chou, S. Chaurasia, Y. S. Wen, J. T. Lin and C. F. Yao, *Chem. Asian J.*, 2012, **7**, 1074; d) S. R. Li, C. P. Lee, H. T. Kuo, K. C. Ho and S. S. Sun, *Chem. Eur. J.*, 2012, **18**, 12085. e) L. Cabau,L. Pellejà,J. N. Clifford, C. V. Kumara, E. Palomares, *J. Mater. Chem. A*, 2013, **1**, 8994.
7 a) C. Olivier, F. Sauvage, L. Ducasse, F. Castet, M. Grätzel and T. Toupance, *ChemSusChem*, 2011, **4**, 731; b) M. F. Xu, M. Zhang, M. Pastore, R. Z. Li, F. D. Angelis and P. Wang, *Chem. Sci*, 2012, **3**, 976; c) N. Cai, R. Z. Li, Y. L. Wang, M. Zhang and P. Wang, *Energy Environ. Sci.*, 2013, **6**, 139; d) Y. Hua, B. Jin, H. D. Wang, X. J. Zhu, W. J. Wu, M. S. Cheung, Z. Y. Lin, W. Y. Wong and W. K. Wong, *J. Power. Sources*, 2013, **237**, 195; e) Y. Hua, S. Chang, D. D. Huang, X. Zhou, X. J. Zhu, J. Z. Zhao, T. Chen, W. Y. Wong and W. K. Wong, *Chem. Mater.*, 2013, **25**, 2146. f) Z. S. Huang, H. L. Feng, X. F. Zang, Z. Iqbal, H. P. Zeng, D. B. Kuang, L. Y. Wang, H. Meierd, D. R. Cao, *J. Mater. Chem. A*, 2014, **2**, 15365.
8 a) Y. Z. Wu, X.Zhang, W. Q. Li, Z. S.Wang, H.Tian, W. H. Zhu, *Adv. Energy Mater.*, 2012, **2**, 149. b) S. Haid, M.Marszalek, A.Mishra, M.Wielopolski, J. Teuscher, J. E. Moser, R. Humphry-Baker, S. M. Zakeeruddin, *Adv. Funct. Mater*., 2012, **22**, 1291.
9 a) X. F. Lu, Q. Y. Feng, T. Lan, G. Zhou, Z. S. Wang, *Chem. Mater*. 2012, **24**, 3179. b) K. Pei, Y. Z. Wu, A. Islam, Q. Zhang, L. Y. Han, H. Tian, W. H. Zhu, *ACS Appl Mater. Interfaces*, 2013, **5**, 4986.
10 W. J.Ying, F. L.Guo, J.Li, Q.Zhang, W. J.Wu, H.Tian, J. L. Hua, *ACS Appl. Mater. Interfaces*, 2012, **4**, 4215.
11 a) S. Y. Qu, W. J. Wu, J. L. Hua, C. Kong, Y. T. Long and H. Tian, *J. Phys. Chem. C*, 2010, **114**, 1343; b) S. Yu, C. Qin, A. Islam, Y. Wu, W. Zhu, J. Hua, H. Tian and L. Han, *Chem. Commun*., 2012, **48**, 6972.
12 Y. Z.Wu, W. H. Zhu, *Chem. Soc. Rev*., 2013, **42**, 2039.
13 a) Y. Sun, S. C. Chien, H. L. Yip, Y. Zhang, K. S. Chen, D. F. Zeigler, F. C. Chen, B. P. Lin and A. K. Y. Jen, *J. Mater. Chem.*, 2011, **21**, 13247; b) N. Blouin, A. Michaud, D. Gendron, S. Wakim, E. Blair, R. Neagu-Plesu, M. Belletete, G. Durocher, Y. Tao and M. Leclerc, *J. Am. Chem. Soc.*, 2008, **130**, 732. c) G. C. Welch, L. A. Perez, C. V. Hoven, Y. Zhang, X. D. Dang, A. Sharenko, M. F. Toney, E. J. Kramer, T. Q. Nguyen and G. C. Bazan, *J. Mater. Chem.*, 2011, **21**, 12700.
14 Y Hua, H. D. Wang, X. J. Zhu, A. Islam, L. Y, Han, C. J. Qin, W. Y. Wong and W. K. Wong, *Dyes Pigm*. 2014, **102**, 196.
15 a)Y. Ooyama and Y. Harima, *ChemPhysChem*, 2012, **13**, 4032. b) S. Chaurasia, C. Y. Hsu, H. H. Chou, J. T. Lin, *Org. Electron*. 2014, **15**, 378. c) X. F. Lu, Q. Y. Feng, T. Lan, G. Zhou, Z. S. Wang, *Chem. Mater*. 2012, **24**, 3179.
16 a) H. H. Chou, Y. C. Chen, H. J. Huang, T. H. Lee, J. T. Lin, C. Tsaic, K. Chen, *J. Mater. Chem.*, 2012, **22**, 10929. b) Q. Wang, J. E.Moser, M.Grätzel, *J. Phys. Chem. B*, 2005, **109**, 14945. c) Y Hua, S Chang, H. D. Wang, D. D. Huang, J. Z. Zhao, T. Chen, W. Y. Wong, W. K. Wong and X. J. Zhu, *J. Power. Sources*, 2013, **243**, 253.d) C. J. Yang, Y. J. Chang, M. Watanabe, Y. Son. Hon and T. J. Chow, *J. Mater. Chem.*, 2012, **22**, 4040. d) J. Shi, J. N. Chen, Z. F. Chai, H. Wang, R. L. Tang, K. Fan, M. Wu, H. W. Han, J. G. Qin, T. Y. Peng, Q. Q. Li, Z. Li, *J. Mater. Chem.*, 2012, **22**, 18830.
17 R. Z. Li, J. Y. Liu, N. Cai, M. Zhang, P. Wang, *J. Phys. Chem. B*, 2010, **114**, 4461.

Table of Content Page

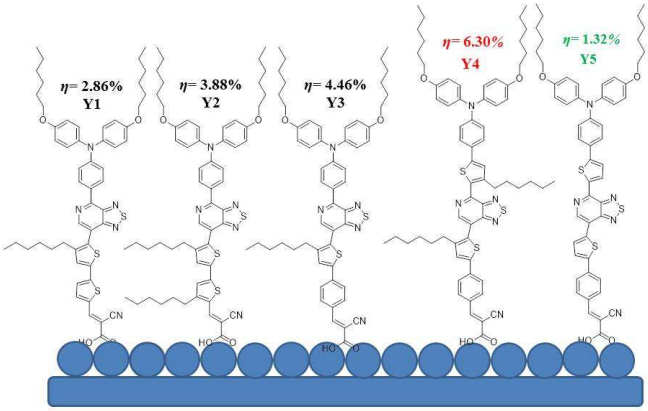

A series of thiadiazolo[3,4-c]pyridine-cored metal-free panchromatic organic sensitizers has been designed for DSSC applications. Their structures, photophysical and electrochemical properties were finely tuned with various π-conjugated spacers, which dramatically enhanced the cell efficiency to 6.30% from 2.86%.

Yong Hua, Jian He, CaishunZhang, ChunjiangQin, LiyuanHan, Jianzhang Zhao, Tao Chen, Wai-Yeung Wong, Wai-Kwok Wong and Xunjin Zhu

Effects of Various π-Conjugated Spacers in Thiadiazole[3,4-c]pyridine-Cored Panchromatic Organic Dyes for Dye-Sensitized Solar Cells

Journal of Materials Chemistry A **2014**, xx, xxxx

